Garone A, Barbieri M, Summa G./ Senses Sci 2014; 1 (4):123-130
doi: 10.14616/sands-2014-4-123130

Hydrogeochemical characterization of the southern sector of the Alburni Massif, Campania region, Italy

Angelica Garone[1], Maurizio Barbieri[1]*, Gianpietro Summa[2]

[1] Department of Earth Science, Sapienza University of Rome, P.le A. Moro, 5 – 00185 Rome, Italy
[2] ARPAB - Agenzia Regionale per la Protezione dell'Ambiente di Basilicata, Via della Fisica 18 C/D - 85100 Potenza, Italy

*Corresponding author: Prof. Maurizio Barbieri, Department of Earth Science, Sapienza University of Rome, P.le A. Moro, 5 - 00185 Rome, Italy, Tel.: +39-06 4991 4593; e-mail: maurizio.barbieri@uniroma1.it

Article history
Received: November 20, 2014
Accepted: December 2, 2014
Published: December 9, 2014

Abstract

The Alburni Massif represents one of the most important karst regions of the Southern Apennines, and it has a high potential as a water resource. This paper reports a hydrogeochemical evaluation of sampled waters from the southern sector of the Alburni Massif (Campania region, Italy). Five water samples were analysed (three from natural springs and two from wells) to i) evaluate the hydrogeochemical properties of the waters in the study area and ii) understand the groundwater flow in this system. Waters sampled were classified as Ca-HCO_3 due to enrichment from different alkaline elements (Na^+ + K^+) and carbonate (HCO_3^- + CO_3^{2-}). This classification is in agreement with the lithologies present in this area. Groundwater flow was connected to the fault line passing through the south-west sector of the complex, which divides the Massif into two large structures situated to the east and the west.

Keywords: *Hydrogeochemical characterization, trace elements, groundwater flow, Alburni Massif*

Introduction

The Alburni Massif represents one of the most important karst areas in Italy. It is located in the Cilento and Vallo di Diano National Park, which was founded on December 6, 1991 through Law No. 334. In 1973, the necessity of protecting the coast and inland areas from speculation and mass tourism was discussed at the International Conference on Mediterranean Coastal Parks. One result of this conference was the establishment of two nature reserves by the Minister of the Environment, Mt. Cervati and Calore River, respectively. The combined area of these two reserves totalled 36,000 ha. The National Park now covers an area of approximately 180,000 ha and includes eight mountain communities and 80 municipalities. The National Park is bordered by the Sele Valley to the north, the Diano Valley to the east, Policastro Gulf to the south and the Tyrrhenian Sea to the west. In 1991, this area was declared an UNESCO Word Heritage Site to protect the temples of Paestum and Certosa of Padula. In 1997, the National Park also became part of a prestigious network of "Biosphere Reserves," which are designated to maintain an equilibrium between man and his environment through the conservation of biological diversity, the promotion of economic development and the preservation of cultural values. Within the Park, the Alburni Massif is an area that takes its name from the highest peak (1742 m a.s.l.) in the group. The northern slope of the peak is steep, while the southern slope has a moderate gradient and hosts beech, turkey oak, deciduous forest and meadows dotted with karst features. The Alburni Massif is characterized by a dense arrangement of karst features throughout the highest elevations of the Central and Southern Apennines [1, 2]; these features are related to the tectonic and geomorphic evolution of the Massif.

The aims of this study are: i) to perform a geochemical evaluation of the waters in the southern sector of the Alburni Massif; and ii) to understand the groundwater flow in this system.

2. Geological framework

The Alburni Massif is included in topographic sheets No. 198 (Eboli) and 199 (Potenza) of the Italian Geological Map (1:100000; Figure 1).

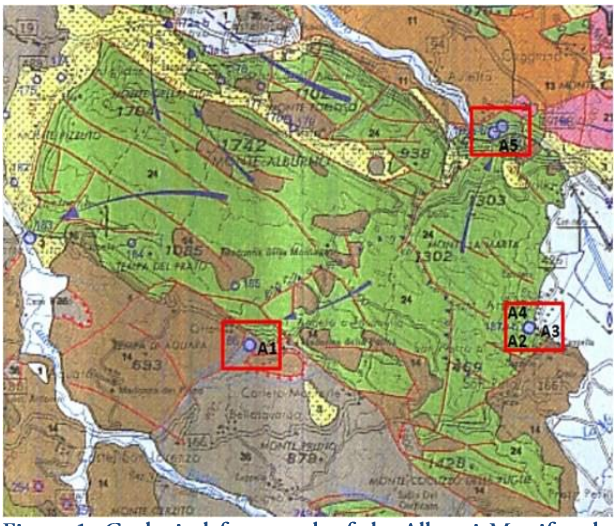

Figure 1. Geological framework of the Alburni Massif and location of sampling sites (red squares).

The Alburni Massif covers an area of approximately 280 km^2 and is bordered by major marginal faults responsible for the subrectangular shape and created a large plateau (average altitude approximately 1300 m a.s.l.) [2]. It is located between the Vallo di Diano to the east, the Tanagro Valley to the north-east, the Calore Valley to the south-west and Sele Valley to the north-west. It is characterized by limestone sequences in carbonate platform facies followed by silicoclastic deposits in flysch facies; locally, especially along the edges, there are continental Quaternary formations. The complete stratigraphic sequence is as follows [3, 4, 5, 6, 7, 8, 9, 10]: a) Mesozoic limestone, b) Tertiary limestone, c) residual red clay, d) flysch deposits, e) sicilide deposits and f) continental Quaternary formations. The carbonate Massif represents a hydrogeological structure characterized by autonomous groundwater circulation. Outcropping rocks can be grouped into four hydrogeological complexes, each with a different permeability. From bottom to top, they are: a) the carbonate complex, characterized by limestone and dolomite; it outcrops in all study areas, is characterized by different fault and fracture systems and has a high permeability; b) the flysch complex, characterized by clays, marls and arenaceous deposits with varying permeabilities; c) the detrital complex with variable permeability due its porosity and d) the lacustrine–alluvial complex, characterized by lacustrine and fluvial deposits. Celico has been found [11] that water flows preferentially from the south-east to the north-west; the major obstacle to this flow is the tectonic line corresponding with the incision between the towns of Pertosa and San Rufo. In this sector, compression traces divide the Alburni Massif into two hydrogeological structures (Figure 2) [12].

Figure 2. Hydrogeological maps of the Alburni Massif (from [12]).

The structure located to the east of this fault drains groundwater toward the Pertosa springs (average flow rate 1.1 cm/sec), while the hydrogeological structure located to the west of the fault drains toward the low-lying Tanagro and Castelcivita springs.

Figure 3 shows a schematic sketch of the hydrological relationships in the southern sector of the Alburni Massif [13]. A perched water table and basal aquifer are present and supply water to different springs and wells located in the study area.

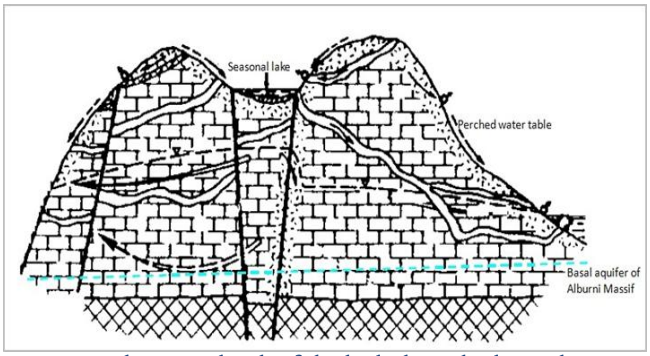

Figure 3. Schematic sketch of the hydrological relationships in the southern sector of Alburni Massif (modify from [13]).

3. Materials and methods

The geochemistry of the southern sector of the Alburni Massif was investigated by sampling three springs and two private wells. The sampling was performed during January and March 2009. In the first month, samples were collected under variable weather conditions and after copious rains, while in March the samples were

taken in sunny weather conditions. In both cases, the sampling period coincided with the charging time of the hydrologic cycle. Groundwater samples were collected at five sites (Table 1).

Table 1. Groundwater sampled in the southern sector of the Alburni Massif. Altitude in meters (m asl) S: spring W: well n.a.: data not available.

Sample	Altitude	Note
A1	280	S
A2	n.a.	W
A3	n.a.	W
A4	475	S
A5	220-263	S

All samples were collected in laboratory certified clean bottles and labelled with the well depth and location, date and time of sample collection, analyses to be performed and field preservation performed, if any [14]. Water temperature, electrical conductivity and pH values were determined in the field. Bicarbonate was determined by titration with 0.1 N HCl using methyl orange and the colour turning method [15]. Water samples were filtered through cellulose filters (0.45 μm), and their major and minor constituents were determined with a Dionex DX-120 ion chromatograph (reliability ±2%). A Dionex CS-12 column was used for determining cations (Na^+, K^+, Mg^{2+}, Ca^{2+}), whereas a Dionex AS9-SC column was used for anions (F^-, Cl^-, NO_3^-, NO_2^-, SO_4^{2-}) [15, 16].
Trace element concentrations were measured using ICP-MS (X Series 2 Thermo Fisher Scientific); the analytical accuracy of these methods ranged from 2% to 5%. All analyses were conducted in the Earth Science Department, "Sapienza" University of Rome, Italy.

4. Results

4.1 Chemical – physical parameters

The physico-chemical characteristics of the groundwater from the southern sector of the Alburni Massif are reported in Table 2.

Temperature values ranging from 9.5 (A4) and 11.9 °C (A5); this range of temperature is typical of the sampling period. The pH of the groundwaters ranged between 7.58 (A3) and 8.19 (A1).

At the end, the electrical conductivity (EC) values ranging from 170 (A4) and 300 μS/cm (A1, A3 and A5).

4.2 Trace elements

Trace element concentrations are reported in Table 3 in accordance with Legislative Decree 152/2006 of National Law.

5. Discussion

5.1 Chemical – physical parameters

In our climate, the pH of natural waters is generally between 7.2 and 7.5. In this case study, the pH values of all samples were greater than average. This is likely the result of an interaction between the water sampled and the limestone it circulated through. As the water circulated, the pH assumed values linked to the equilibrium of the system $CO_2 – H_2O – CaCO_3$, which regulated by the partial pressure of carbon dioxide in the gas phase and temperature.
The ionic dominance pattern of the water samples for cations and anions was $Ca^{2+} > Na^+ > Mg^{2+} > K^+$ and $HCO_3^- > Cl^- > NO_3^- > SO_4^{2-} > F^- > NO_2^-$, respectively. The high concentrations of Ca^{2+} and HCO_3^- are connected to the geology of the study area; the sampling sites belong to an important karst system, where calcite dissolution is an important process that leads to the formation of the HCO_3^- ion (soluble) and the subsequent release of Ca^{2+}.

5.2 Hydrogeochemistry

The relative abundance of major elements allows us to identify the only geochemical family found, as shown in the Langelier-Ludwig diagram (Figure 4). Tested waters have the Ca-HCO_3 chemical composition as a result of the different enrichment rates of water in alkaline elements ($Na^+ + K^+$) and carbonate ($HCO_3^- + CO_3^{2-}$).

Figure 4. Ludwig-Langelier diagram of the waters collected in the southern sector of the Alburni Massif.

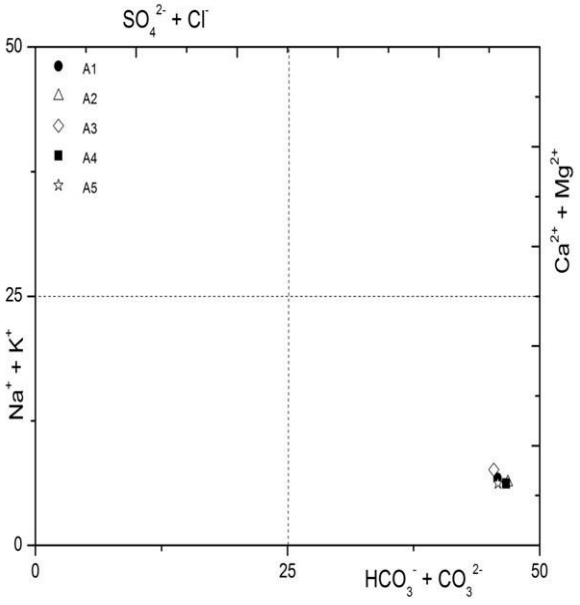

The samples are homogeneous and consist of only one water type, the composition of which is substantially linked to the lithology of the site examined.

The Schoeller diagram below (Figure 5) illustrates a more detailed characterization of each sample's hydrogeochemistry; this diagram highlights slight anomalies between samples because it is based on the direct relationship of the ionic concentrations (expressed in meq/L).

As shown in Figure 5, the waters drawn have similar hydrogeochemical characteristics, and all samples have a calcium-bicarbonate geochemical profile typical of waters circulating in carbonate rocks. In fact, each sample contains high concentrations of Ca^{2+} and HCO_3^-. The sampling sites belong to an important karst system; in this system the calcite dissolution is an important process that leads to the formation of the HCO_3^- ion and the subsequent release of Ca^{2+}. The presence of HCO_3^- is also related to the existence of carbon dioxide, both in deep waters and the infiltration zone. Bicarbonate concentrations increase at low temperatures (with the increase of the CO_2 solubility in water) and where the CO_2 production is high (due to the agricultural practices). Aquifer leaching and low salinity concentrations, along with an increase in bicarbonate concentrations over sulphates and chlorides, prevail in the regional climate. However, in the karst regions of our

Table 2. Chemical and physical parameters of groundwater samples for the Alburni Massif area. Temperature (T) in °C, electrical conductively (EC) in µS/cm, Ca^{2+}, Mg^{2+}, Na^+, K^+, Cl^-, SO_4^{2-}, HCO_3^-, F^-, NO_2^- and NO_3^- in mg/L.

Sample	T	pH	EC	Ca^{2+}	Mg^{2+}	Na^+	K^+	Cl^-	SO_4^{2-}	HCO_3^-	F^-	NO_2^-	NO_3^-
A1	10.8	8.19	300	49.5	3.05	8.84	1.56	5.29	5.93	183	0.08	0.06	1.73
A2	9.6	7.82	180	40.0	0.94	5.94	1.65	3.07	2.96	134	0.06	0.00	1.27
A3	11.3	7.58	300	42.9	1.80	8.30	1.90	6.37	3.39	153	0.07	0.00	4.42
A4	9.5	8.01	170	40.6	0.83	5.84	1.68	30.7	2.78	48.8	0.62	0.00	15.1
A5	11.9	7.67	300	51.3	10.1	9.56	2.62	7.29	4.83	207	0.13	0.13	6.02

Table 3 (Continued). Trace elements in groundwater samples of the Alburni Massif area

Sample	Li	B	V	Cr	Mn	Fe	Co	Ni	Cu	Zn
Lgs.D. 152/2006	ppb	ppb	ppb	ppb	ppb	ppb	ppb	ppb	ppb	ppb
MAC (in ppb)		1000	50	50				20		
A1	0.02	<0.01	0.59	0.30	0.19	1.98	0.09	1.32	2.30	13.3
A2	0.08	1.07	0.64	0.56	0.98	7.58	0.12	0.19	0.35	5.22
A3	0.02	<0.01	0.52	0.21	0.03	4.06	0.09	0.33	1.48	3.22
A4	0.63	9.55	1.26	0.58	2.92	16.8	0.11	0.61	0.36	5.68
A5	0.22	1.77	0.86	0.26	1.93	14.7	0.12	0.43	0.48	1.68

Sample	Ga	As	Rb	Sr	Cd	Sb	Cs	Ba	Hg	Tl	Pb
Lgs.D. 152/2006	ppb	ppb	ppb	ppb	ppb	ppb	ppb	ppb	ppb	ppb	ppb
MAC (in ppb)		10			5				1		10
A1	0.02	0.24	2.68	41.4	0.06	0.07	0.01	158	0.58	<0.01	0.02
A2	<0.01	0.84	1.81	77.1	0.02	0.07	0.02	78.6	0.32	<0.01	0.22
A3	0.01	0.20	1.87	41.2	<0.01	0.03	<0.01	31.8	0.24	<0.01	<0.01
A4	0.02	1.16	2.40	101	0.33	0.23	0.03	77.5	0.10	0.01	3.45
A5	0.04	0.32	1.98	74.6	0.14	0.13	0.02	24.1	0.70	0.01	1.93

study site, this zoning is not entirely valid because the water is removed quickly from the surface and circulates at depth, where it takes on the characteristics of the aquifer. The Schoeller diagram provides additional information on the groundwaters sampled. The lines of A1 and A3 are similar, except for the Cl/SO_4 molar ratio (Figure 6).

Figure 5. Schoeller diagram representing the waters collected in the Alburni Massif area.

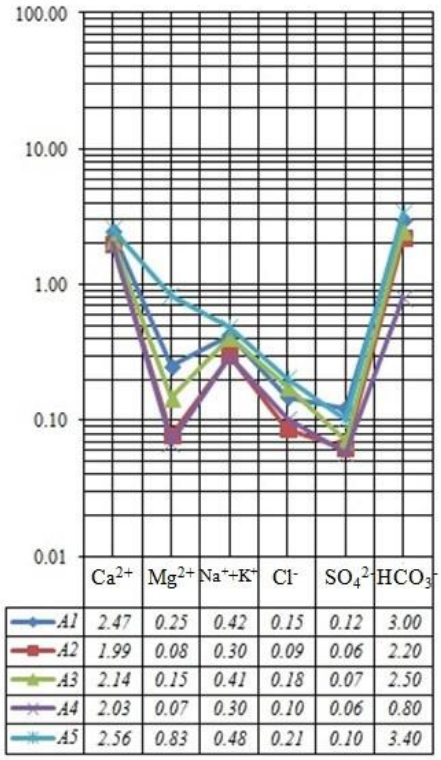

	Ca^{2+}	Mg^{2+}	$Na^{+}+K^{+}$	Cl^{-}	SO_4^{2-}	HCO_3^{-}
A1	2.47	0.25	0.42	0.15	0.12	3.00
A2	1.99	0.08	0.30	0.09	0.06	2.20
A3	2.14	0.15	0.41	0.18	0.07	2.50
A4	2.03	0.07	0.30	0.10	0.06	0.80
A5	2.56	0.83	0.48	0.21	0.10	3.40

The A3 well is located at approximately the same altitude as the A1 spring and draws on the highest part of the basal aquifer. According to vertical hydrochemical zonation, the A3 well extends into bicarbonate facies, and its waters are bicarbonate. However, the A1 spring receives water contributions from the upper (fast flow) and the deep (slow flow) part of the aquifer. The slower circulation of water at depth allows for its enrichment via more soluble, though less abundant, salts in solution. This enrichment can be explained in two ways: a) greater vertical hydrochemical zonation (the A1 spring extends into the sulphate facies) and b) saturation of the more soluble salt in solution. These phenomena explain the A1 spring water's higher sulphate concentration compared to A3 well.

A comparison of the data from the A2 well and A4 spring (Figure 7) shows almost identical results, although the sample sites were located at different altitudes (470 m a.s.l. and 475 m a.s.l., respectively).

Both the well and the spring draw from the same shallow groundwater, which is characterized by rapid flow and leaches the same type of rocks. The vertical hydrochemical zonation does not vary between the two water samples, which have a homologous supply mode from the same aquifer.

Sample A5, as shown in Figure 8, is dissimilar with respect to the others.

Figure 6. Schoeller diagram for samples A1 and A3.

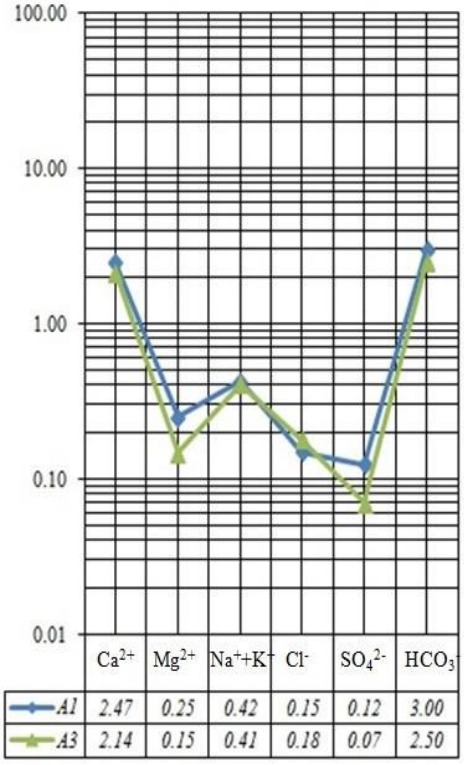

	Ca^{2+}	Mg^{2+}	$Na^{+}+K^{+}$	Cl^{-}	SO_4^{2-}	HCO_3^{-}
A1	2.47	0.25	0.42	0.15	0.12	3.00
A3	2.14	0.15	0.41	0.18	0.07	2.50

This sample also belongs to the bicarbonate type, but it has a higher Mg^{2+} concentration and lower Na^{+} and K^{+} concentrations than the other samples. The higher Mg^{2+} concentration is likely linked to the lithology of the substrate at depth (may be dolomitic-limestone and dolomite). While there are not dolomite formations in this area of the Alburni Massif, the high Mg^{2+} concentration in the sample indicates extended circulation of the water at depth and its contact with dolomitic-limestone at the basement of the carbonate stack. This hypothesis is justified by the higher Na+ and K^{+} concentrations in the A5 sample compared to the concentrations of these ions in the other samples.

5.3 Trace elements

The analysis of minor and trace elements in natural waters has improved substantially following the development of new analytical methodologies that provide better quality measurements. Environmental

geochemistry reveals that the continuous introduction of many trace elements into the environment via atmospheric and hydrological cycles has been strongly disturbed by human activity [17, 18]. In addition, a number of natural processes (e.g., volcanic activity, chemical weathering of crustal rocks, etc.) help to determine concentrations of unwanted and/or harmful metals in water.

Figure 7. Schoeller diagram for samples A2 and A4.

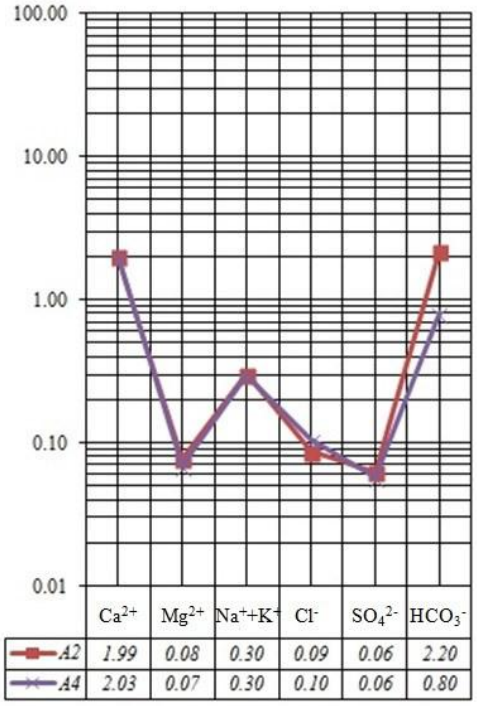

In view of the strong toxicity of many metals, the presence of trace elements and potential pollutants cannot be disregarded from this analysis. From a purely environmental point of view, and with reference to the Maximum Allowable Concentrations (MAC) for various elements defined in Legislative Decree 152/2006, no minor or trace elements exceed their threshold values.

Sr^+ is the only element with a high concentration, but it has no threshold value. This element is an alkaline earth metal and was discovered in 1789 by Adair Cramford. It has a chemical structure similar to calcium and can replace it in some cases.

Figure 9 shows the distribution of Sr^{2+} with relation to the pH of measured samples.

Water-rock interaction (WRI) processes justify the general positive correlation between Sr^+ concentrations and pH for samples A2, A3 and A4. The increase of pH and Sr^+ concentrations can be explained by a prolonged interactions between the groundwater and sediments/rocks.

Figure 9 also shows the calcite ($CaCO_3$) dissolution line at pH value of 7.8; under this line, the solution is undersaturated with respect to $CaCO_3$, while above the line the solution is oversaturated with respect to $CaCO_3$.

The A1 sample is located in the oversaturated sector; it's characterized by a low Sr^+ concentration and the highest pH value of the samples examined. $CaCO_3$ dissolution causes the release of Ca^{2+}, HCO_3^- and OH^- ions; as a consequence, a higher concentration of Ca^{2+} exists in solution compared to Sr^+. The pH value of the A1 sample should be relatively lower than the other samples' measured values, but the opposite occurs. This can be explained by the presence of a higher concentration of dissolved oxygen in the water, which reacts with H_3O^+ ions and lowers their concentration, resulting in a higher measured pH.

Figure 8. Schoeller diagram for sample A5.

Sample A5 falls in the undersaturated $CaCO_3$ sector of the graph; this means that at this site, free Ca^{2+} ions exist in low concentration. Additionally, the pH value is high and, consequently, the concentration of Sr^+ increases.

6. Conclusions

The present study aimed to develop a hydrogeochemical profile of the waters located along the southern sector of the Alburni Massif. A geochemical campaign was conducted in January 2009 at five selected sites (three springs and two wells).

Through this study, the waters sampled were identified as Ca-HCO_3 a result of enrichment in alkaline elements (Na^+ + K^+) and carbonate (HCO_3^- + CO_3^{2-}) common to the lithologies of the area. The sites examined belong to an important karst system, where the calcite dissolution is an important process that leads to

the formation of the HCO_3^- ion (soluble) and the subsequent release of Ca^{2+}.

Figure 9. Diagram of Sr^{2+} vs. pH for groundwaters of the Alburni Massif.

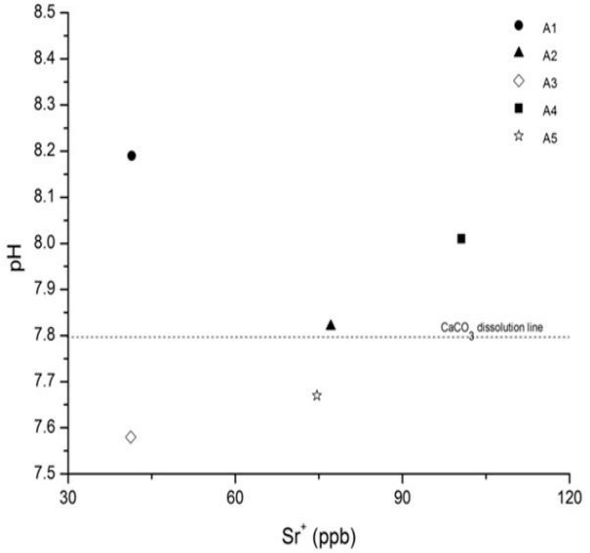

Groundwater flow within the Alburni Massif is connected to the fault line passing through its south-west sector.

This fault line divides the Massif into two large structures situated to the east and west, which drain the waters from the basement to the Pertosa springs and Tanagro and Castelcivita springs, respectively.

The Alburni Massif is an important carbonate complex on the edge of Cilento; Cilento possesses few water resources, and in the summer, water demand exceeds availability. Interest in the Alburni Massif mountain complex stems from its potential as a water resource. A management plan should be arranged to protect this water resource, including:

- Qualitative and quantitative monitoring of different springs in this area;
- Analysis to define natural water availability;
- Assessment of the impact of human activity;
- Designation of quality objectives and the organization of a refined sustainability management plan for the study area.

References

1. Brancaccio L, Civita M, Vallario A. Prime osservazioni sui problemi idrogeologici dell'Alburno (Campania). Boll. Soc. Nat., 1973; 82, 13-35
2. Bellucci F, Giulivo I, Pelella G, SANTO A. Monti Alburni. Ricerche speleologiche. 1995; 13-26.
3. Sartoni S, Crescentini U. Ricerche biostratigrafiche nel Mesozoico dell'Appennino meridionale. Giorn. Geol., 1962; s. 2, 29, Bologna.
4. Bravi S, Schiattarella M. Segnalazione dei livelli ittiolitici eocenici a Cyclopoma gigas Agassiz nei Monti Alburni (Appennino Campano). Soc. Natur. Napoli, 1988; 95, 255-279.
5. Boni V. Le argille rosse continentali del passaggio Paleocene-Miocene della piattaforma carbonatica campano-lucana. Boll. Soc. Geol. Ital. 1974; 1059-1094.
6. Santo A. Le ruditi dei Monti Alburni nel quadro dell'evoluzione alto-miocenica dell'Appennino campano. Boll. Soc. Geol. It.; 1995.
7. Pescatore T, Scandone P, Sgrosso I. Lineamenti di geologia dei Monti Alburni. Atti "Incontri Internazionali di Speleologia" Salerno, 1972; 13-17.
8. Ascione A, Cinque A, Santangelo N, Tozzi M. Il bacino del Vallo di Diano e la tettonica trascorrente Plio-quaternaria: nuovi vincoli cronologici e cinematici. Studi Geologici Camerti, volume speciale 1992/a; 201-208.
9. Santangelo N. Evoluzione stratigrafica, geomorfologica e neotettonica di alcuni bacini lacustri del confine campano-lucano (Italia meridionale). Tesi di dottorato, Dip. Scienze della Terra, Università di Napoli, 1990.
10. Ascione A, Cinque A. Il margine nord-orientale degli Alburni. Guida all'escursione: evoluzione geomorfologica e tettonica quaternaria dell'Appennino centro-meridionale. Dipartimento di Scienze della Terra di Napoli, 1992.
11. Celico P. Schema idrogeologico dell'Appennino carbonatico centro-meridionale. Mem. e note dell'Ist. Di Geol. Appl., 1978/a; 14.
12. Celico P., Pelella L, Stanzione D, Aquino S. Sull'idrogeologia e l'idrogeochimica dei Monti Alburni (SA). Geologica Romana, 1994; 30, 687-698.
13. Summa G. Relazione idrogeologica. Area in esame: comuni di Sant'Arsenio (SA) e San Pietro al Tanagro (SA).
14. APHA, "Standard Methods for the Examination of Water and Wastewater," 19th Edition, American Public Health Association, Washington DC, 1995.
15. Barbieri M, Battistel M, Garone A. The geochemical evolution and management of a coastal wetland system: a case study of Palo Laziale protected area. J Geochem Explor, 2013; 126-127: 67-77.
16. Abbas M, Barbieri M, Battistel M, Brattini G, Garone A, Parisse B. Water quality in the Gaza Strip: the

present scenario. J Water Res Prot, 2013; 5: 54-63.
17. Forstner U & Wittman G.T.V. Metal pollution in the aquatic environment. Springer – Verlag, Berlin, 1984.
18. Solomons W & Forstner U. Metal in the hydrocicle. Springer – Verlag, Berlin, 1984.